

Spectral Evolution of a Luminous Compact X-Ray Source in NGC 253 with Chandra and XMM-Newton *

Takaaki TANAKA,^{1,2} Masahiko SUGIHO,² Aya KUBOTA,³ Kazuo MAKISHIMA,^{2,3}
and Tadayuki TAKAHASHI^{1,2}

¹*Institute of Space and Astronautical Science, JAXA, 3-1-1 Yoshinodai, Sagami-hara, Kanagawa 229-8510*
ttanaka@astro.isas.jaxa.jp

²*Department of Physics, The University of Tokyo, 7-3-1 Hongo, Bunkyo-ku, Tokyo 113-0033*

³*RIKEN, 2-1 Hirosawa, Wako, Saitama 351-0198*

(Received 2004 December 3; accepted 2005 February 28)

Abstract

Spectral studies of a luminous X-ray source, NGC 253 X21, are presented based on archival Chandra and XMM-Newton data. The Chandra observation on 1999 December 16 detected the source at a bolometric luminosity of 0.3×10^{39} erg s⁻¹ (assuming isotropic emission), while an XMM-Newton observation on 2000 June 3 revealed a short-term source variation in the range of $(0.6\text{--}1.3) \times 10^{39}$ erg s⁻¹. All spectra from these observations were successfully modeled by emission from an optically thick accretion disk. The average inner disk radius was kept constant at $63 \cdot (\cos 60^\circ / \cos i)^{1/2}$ km, where i is the disk inclination, and did not vary significantly, while the disk inner temperature changed in the range of 0.9–1.4 keV. Assuming that this object is an accreting Schwarzschild black hole, and that the disk inner radius coincides with its last stable orbit, the mass of the black hole is estimated to be $\sim 7 M_\odot$. The disk luminosity corresponds to $(30\text{--}120) \cdot (\cos 60^\circ / \cos i)$ % of the Eddington limit of this black hole. Therefore, this luminous X-ray source, NGC 253 X21, is understood consistently to be an accreting stellar mass black hole in the standard disk state.

Key words: accretion, accretion disks — black hole physics — galaxy: individual (NGC 253)

1. Introduction

Since the era of the Einstein Observatory, many compact X-ray sources have been detected in nearby galaxies (e.g., Fabbiano 1989). Sources with X-ray luminosities below $\sim 2 \times 10^{38}$ erg s⁻¹, which corresponds to the Eddington limit for a neutron star of $1.4 M_\odot$, can be accreting neutron stars, while those with higher luminosities can be considered as black hole binaries (hereafter, BHB). The most luminous class of compact objects, known as ultra-luminous compact X-ray sources (ULXs; Makishima et al. 2000), show X-ray luminosity of $\sim 10^{39}\text{--}10^{40}$ erg s⁻¹. Supposing that ULXs obey the Eddington limit, their high luminosities imply that they are accreting black holes as massive as $10\text{--}100 M_\odot$ or more. Such luminous X-ray objects, which are rather rare in our Galaxy and LMC, are suggested to reside preferentially in galaxies with high star-formation activities (Gilfanov et al. 2004). Therefore, starburst galaxies provide a good opportunity to study stellar black holes of various masses.

In studying Galactic/Magellanic BHBs, intensity-correlated spectral changes have been used as a key diagnostic tool. When the luminosity is above $\sim 3\%$ of the Eddington limit, a BHB is often in the standard-disk (alternatively called high or soft) state, wherein the X-ray spectrum is successfully described by a so-called multi-

color disk model (MCD model; Mitsuda et al. 1984), predicted by the theory of optically thick standard accretion disks (Shakura, Sunyaev 1973). The bolometric disk luminosity, L_{disk} , varies as $\propto T_{\text{in}}^4$, where T_{in} is the highest color temperature of the disk. Equivalently, the calculated innermost disk radius, R_{in} , stays constant, at a value consistent with the radius of the last stable orbit around the black hole. As the source becomes more luminous (close to the Eddington limit), R_{in} apparently becomes variable, as $R_{\text{in}} \propto T_{\text{in}}^{-1}$, probably because the disk makes a transition into a slim disk (Kubota et al. 2001; Kubota, Makishima 2004). A very similar behavior has been observed for several of the most luminous ULXs, which show MCD-like spectra (Mizuno et al. 2001; Sugiho 2003; Kubota et al. 2002). It is therefore of keen interest to look for such intensity-correlated spectral changes among extragalactic BHB candidates, in particular including those with lower luminosities, and to examine whether the behavior indicates standard disks or slim-disks.

With this perspective, we analyzed the XMM-Newton and Chandra data of NGC 253 X21 (Vogler, Pietsch 1999; also named Source 5 in Fabbiano, Trinchieri 1984). The nearby Sc-type edge-on galaxy NGC 253 (at a distance of 2.58 Mpc; Puche, Carignan 1988) is one of the well-known starburst galaxies with prominent diffuse X-ray emission (e.g., Strickland et al. 2002). Many point-like X-ray sources have also been detected since the era of the Einstein Observatory. Among them, X21 is one of the brightest sources, located approximately $4'$ southwest

* Partly based on the observations obtained with XMM-Newton, an ESA science mission with instruments and contributions directly funded by ESA Member States and NASA, USA.

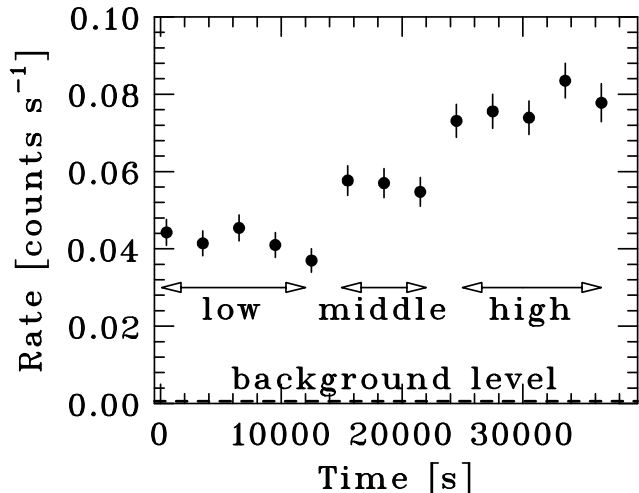


Fig. 1. The 0.5–10 keV light curve of X21 (in counts s^{-1}), averaged over the two MOS cameras of XMM-Newton. The background is not subtracted.

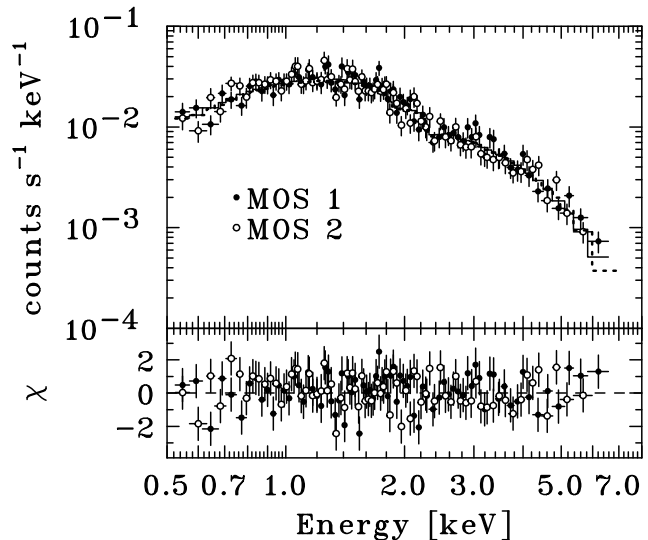


Fig. 2. Time-averaged XMM-Newton spectra of X21, together with the data residuals from the best-fit MCD model.

from the center of this galaxy. Vogler, Pietsch (1999) showed that this source is time-variable by analyzing ROSAT data, and Pietsch et al. (2001) analyzed the XMM-Newton data of X21 and reported that its luminosity varied by a factor of ~ 2 during a 40 ks observation. In a large sample of ULXs observed with Chandra and XMM-Newton (Sugihro 2003), this source showed a large luminosity variation in the range of $\sim 10^{38}$ erg s^{-1} – 10^{39} erg s^{-1} . Therefore, this object deserves a detailed study in comparison with Galactic/Magellanic BHBs.

2. Observations and Data Reduction

The XMM-Newton (Jansen et al. 2001) observation of NGC 253, to be utilized in the present paper, was carried out on 2000 June 3. The data, retrieved from the XMM-Newton archive, were processed using the Science Analysis System (SAS), version 5.4.1. To create response matrices, the software package *rmfgen* was used. Since X21 was located on the CCD gap of the PN detector (Strüder et al. 2001) during the observation, the present paper utilizes only the MOS (MOS 1 and MOS 2; Turner et al. 2001) data. For each EPIC camera, events with pattern 0 to 12 were accumulated over a region of $15''$, centered on the X21 image. A total of 35 ks of good data were obtained for the two MOS cameras by discarding the time region of a short background time flare. Figure 1 shows a 0.5–10 keV light curve with an average count rate of each MOS camera of 0.06 cts s^{-1} , which roughly gives a 0.5–10 keV flux of 1×10^{-12} erg s^{-1} cm^{-2} . As shown by the dashed line at the bottom, the background counts were negligible ($\sim 1\%$ of the source counts in this range). The signal count rate varied by a factor of two, as already reported by Pietsch et al. (2001).

The present work also utilized a Chandra (Weisskopf et al. 2000) observation of NGC 253, performed on 1999 December 16. The Chandra data consisted of a net ex-

posure of 14 ks, when the target source was on the S3 chip. The data reduction was carried out using CIAO software version 2.3, and the response matrix was made with *mkrmf*. The source events were extracted from a circular region of $3''.7$ radius around the source centroid. The average 0.5–10 keV count rate was 0.06 cts s^{-1} , which corresponded to a 0.5–10 keV energy flux of 3×10^{-13} erg s^{-1} cm^{-2} , a factor of three lower than the average flux observed with XMM-Newton. There was no significant time variation beyond the Poisson noise.

3. Analyses and Results

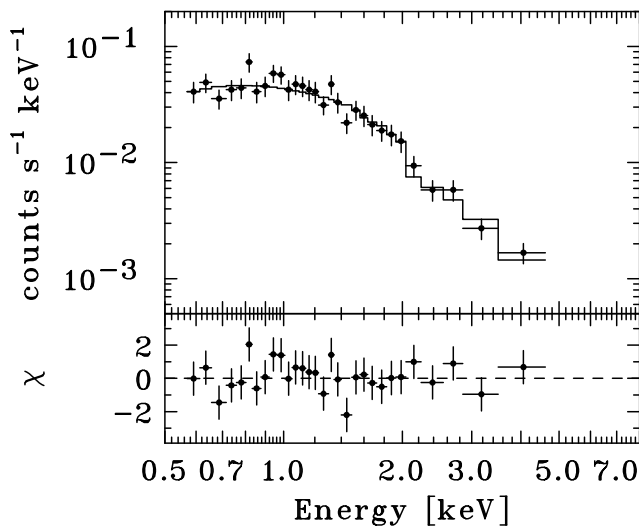
3.1. Averaged Spectra

Figure 2 shows the time-averaged spectra of X21 obtained with the XMM-Newton MOS cameras. The background events were extracted from a source-free circular region of $2'$ radius on the same chip as the source. Following the previous studies on ULXs (e.g. Makishima et al. 2000), the MCD model and a single power law (PL) model were fit to the spectra. As summarized in table 1, the MCD model successfully describes the observed spectra with $\chi^2/\nu = 149.9/152$, while the PL model is less successful with $\chi^2/\nu = 175.9/152$. The value of the hydrogen column density, N_H , obtained with the MCD fit, is roughly consistent with the line-of-sight Galactic value of $N_H = 1.4 \times 10^{20}$ cm^{-2} (Dickey, Lockman 1990), while that with the PL model is by a factor of 20 higher than the Galactic value. Furthermore, the value of N_H estimated from the MCD fit is consistent with the value from a spectral analysis of diffuse emission in this region of NGC 253 reported by Strickland et al. (2000). Thus, the MCD model explains the data more appropriately than the PL model. Employing a correction factor for the inner-boundary condition of $\xi = 0.41$ (Kubota et al. 1998) and a color-to-effective temperature correction factor of $\kappa \sim 1.7$

Table 1. The best-fit parameters of the energy spectra of NGC 253 X21*

Observations	Model	Parameter	N_{H}^{\dagger}	f_x^{\ddagger}	χ^2/ν
XMM-Newton, average	MCD	$T_{\text{in}}^{\S} = 1.28_{-0.06}^{+0.07}$, $R_{\text{in}}^{\parallel} = 59 \pm 6$	6 ± 2	9.38	149.9/152
	Power law	$\Gamma^{\#} = 2.01_{-0.08}^{+0.09}$	27 ± 4	10.7	175.9/152
XMM-Newton, high-flux period	MCD	$T_{\text{in}} = 1.4 \pm 0.2$, $R_{\text{in}} = 60_{-12}^{+16}$	11 ± 7	14.0	27.5/42
XMM-Newton, middle-flux period	MCD	$T_{\text{in}} = 1.3 \pm 0.2$, $R_{\text{in}} = 63_{-16}^{+21}$	6 ± 6	9.47	31.2/33
XMM-Newton, low-flux period	MCD	$T_{\text{in}} = 1.2_{-0.2}^{+0.1}$, $R_{\text{in}} = 60_{-10}^{+13}$	1_{-1}^{+5}	6.37	46.7/49
Chandra, average	MCD	$T_{\text{in}} = 0.9 \pm 0.1$, $R_{\text{in}} = 69_{-14}^{+21}$	2_{-2}^{+4}	3.15	23.8/27
	Power law	$\Gamma = 2.2_{-0.2}^{+0.3}$	20_{-6}^{+7}	3.94	25.4/27

* Errors represent 90% confidence.

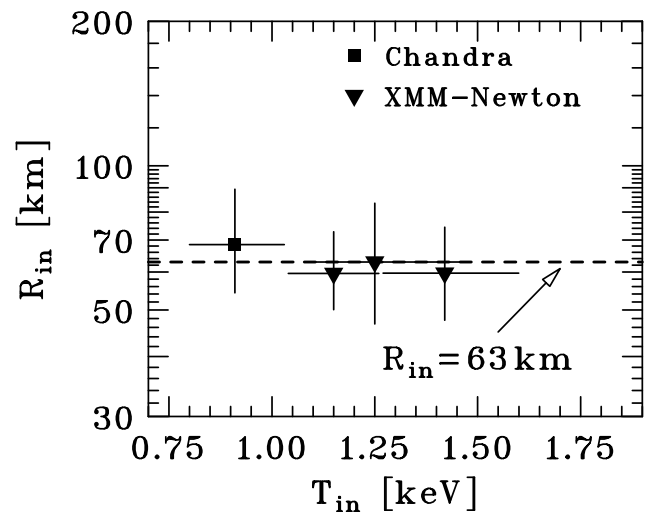
 \dagger Hydrogen column density in the unit of 10^{20} cm^{-2} \ddagger 0.5–10 keV X-ray flux in the unit of $10^{-13} \text{ erg s}^{-1} \text{ cm}^{-2}$. \S In the unit of keV. \parallel In the unit of km. $\#$ Photon index.**Fig. 3.** Chandra ACIS spectrum of X21, together with the best-fit MCD model. The bottom panel shows the fit residuals.

(Shimura, Takahara 1995), the best-fit MCD model yields the innermost disk radius, $R_{\text{in}} = (59 \pm 6) \cdot \zeta^{1/2} \text{ km}$ with $\zeta \equiv \cos 60^\circ / \cos i$, where i is the inclination of the system. By using a formula for the disk bolometric luminosity, L_{disk} , by Makishima et al. (2000),

$$L_{\text{disk}} = 4\pi \left(\frac{R_{\text{in}}}{\xi} \right)^2 \sigma \left(\frac{T_{\text{in}}}{\kappa} \right)^4, \quad (1)$$

where σ is the Stefan–Boltzmann constant, L_{disk} is then calculated as $8.6 \times 10^{38} \cdot \zeta \text{ erg s}^{-1}$, which corresponds to the Eddington limit of a $5.8 M_{\odot}$ object. An MCD plus PL model with a fixed photon index of $\Gamma = 2.0$ gives essentially the same result within 90% errors, because the PL component in this two-component fit is not significant.

The Chandra ACIS spectrum of X21 was analyzed in the same manner. Figure 3 shows the obtained source spectrum, after subtracting the background spectrum, which was extracted from a source-free circular region of $30''$ radius on the same chip as the source. The spec-

**Fig. 4.** Relation between the highest color temperature of the disk (T_{in}) and the calculated innermost disk radius (R_{in}) of NGC 253 X21. The dashed line represents $R_{\text{in}} = 63 \text{ km}$. A disk inclination of $i = 60^\circ$ is assumed.

trum was fit with the MCD model and the PL model, as was done for the XMM-Newton data. As shown in table 1, the spectrum can be described by either model because of the poor statistics. However, the MCD fit is again more reasonable from the viewpoint of N_{H} . The Chandra data thus yield $R_{\text{in}} = (69_{-14}^{+21}) \cdot \zeta^{1/2} \text{ km}$ and $L_{\text{disk}} = 2.9 \times 10^{38} \cdot \zeta \text{ erg s}^{-1}$. Between the XMM-Newton and the Chandra observations, the value of R_{in} was kept almost constant at $\sim 60 \cdot \zeta^{1/2} \text{ km}$, while L_{disk} changed by a factor of three.

3.2. Intensity-Related Change of the Spectrum

As shown in figure 1 and reported by Pietsch et al. (2001), X21 exhibited a significant intensity variation by a factor of two during the XMM-Newton observation. Accordingly, the entire observational span was split into three periods; covering low-flux, middle-flux, and high-flux periods, as denoted by the three arrows in the figure.

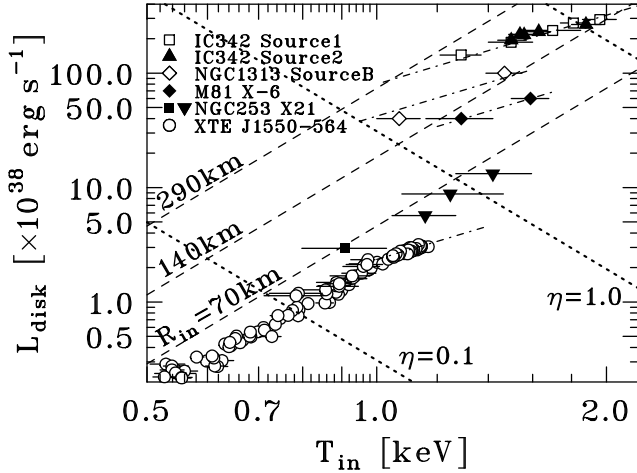


Fig. 5. Scatter plot between the disk bolometric luminosity (L_{disk}) and the highest color temperature (T_{in}) obtained from the MCD-model fit. All data points of NGC 253 X21 refer to the present work. Those of other ULXs, IC 342 Source 1, IC 342 Source 2, M 81 X-6 and NGC 1313 Source B, were obtained with ASCA (Mizuno et al. 2001). The data points of the Galactic BHB, XTE J1550–564, are taken from Kubota, Makishima (2004), and are shifted downward for clarity by a factor of two. The inclination is assumed to be 60° for all data. The dashed lines represent $L_{\text{disk}} \propto T_{\text{in}}^4$, hence mean constant value of R_{in} , and the dot-dashed lines represent $L_{\text{disk}} \propto T_{\text{in}}^2$. The parameter η specifies the disk bolometric luminosity normalized to the Eddington luminosity ($\eta = L_{\text{disk}}/L_{\text{Edd}}$). For NGC 253 X21, the same symbols with figure 4 are used.

Spectra constructed from each period were investigated with the absorbed MCD model to clarify the spectral evolution in response to the intensity change. As shown in table 1, this model reproduced each spectrum very well.

Figure 4 shows the values of R_{in} against T_{in} , based on the intensity-sorted XMM-Newton spectra (filled inverted triangles) and the Chandra spectrum (filled square). It clearly shows that the value of R_{in} remained constant during the significant variation of T_{in} . The data points are consistent with the behavior of BHBs in the standard-disk state, where R_{in} remained constant. The average value of R_{in} is determined as $(63_{-7}^{+9}) \cdot \zeta^{1/2}$ km.

In figure 5, the calculated values of L_{disk} are plotted against T_{in} for each period, in order to examine the spectral behavior against the luminosity. This diagram shows that the data points satisfy the relation $L_{\text{disk}} \propto T_{\text{in}}^4$ as L_{disk} changes over $(0.3\text{--}1.3) \times 10^{39} \cdot \zeta$ erg s $^{-1}$. In fact, a logarithmic slope of 3.6 ± 0.6 is obtained when these data points are fitted with a power law.

4. Discussion

Through the combined use of archival Chandra and XMM-Newton data, an overall luminosity change by a factor of three was observed from NGC 253 X21. The X-ray spectra at all intensity levels were successfully described by the MCD model, and the highest disk luminosity reached $1.3 \times 10^{39} \cdot \zeta$ erg s $^{-1}$. This luminosity, on one

hand, is the lowest among those of ULXs. On the other hand, this source is shining at a higher luminosity than most Galactic/Magellanic sources. Except for a few examples, such as GRS 1915+105 and XTE J1550–564 in its outburst peak, no compact X-ray source in our Galaxy has so far exhibited a luminosity higher than 1×10^{39} erg s $^{-1}$ (e.g., Gierliński, Done 2004; Zycki et al. 1999).

In order to study the spectral behavior of X21 compared with luminous ULXs and XTE J1550–564, which is a representative Galactic BHB, their $T_{\text{in}}\text{--}L_{\text{disk}}$ relations are plotted together in figure 5. While the luminosities of luminous ULXs are observed to vary as $\propto T_{\text{in}}^2$, that of NGC 253 X21 varied as $L_{\text{disk}} \propto T_{\text{in}}^4$. The latter relation is considered to be a signature of standard accretion disks (Shakura, Sunyaev 1973), as has been observed from a fair number of BHBs, including XTE J1550–564, LMC X-3 (Ebisawa et al. 1993), GS 2000+25 (Takizawa 1991), and GS 1124–684 (Ogawa 1992). The present results thus provide one of the first confirmations of the standard-disk property in BHB candidates outside the local group of galaxies.

As shown in Section 3, the value of R_{in} of X21 was estimated to be $63 \cdot \zeta^{1/2}$ km. The innermost stable orbit of a non-rotating BH is given as $3R_{\text{s}}$, where $R_{\text{s}} = 2GM/c^2$ is the Schwarzschild radius. Thus, the mass of the central black hole of this source is estimated to be $7 \cdot \zeta^{1/2} M_{\odot}$. This is a very common value found among BHBs in our Galaxy and LMC (e.g., McClintock, Remillard 2005). Thus, the observed disk luminosity of $(0.3\text{--}1.3) \times 10^{39} \cdot \zeta$ erg s $^{-1}$ corresponds to $(30\text{--}120) \cdot \zeta$ % of the Eddington limit for the inferred BH mass. Therefore, NGC 253 X21 can be understood consistently as an accreting BH with an ordinary stellar mass, in which a standard accretion disk is radiating at a fair fraction of the Eddington limit. In particular, the observed values of $T_{\text{in}} = 0.9\text{--}1.4$ keV are reasonable for the inferred BH mass and luminosity, thus making X21 free from the problem of “too high a disk temperature” observed from the most luminous ULXs (Makishima et al. 2000).

According to the present results, the least-luminous class of the entire ULXs population may contain ordinary BHBs. Similar examples include M 33 X-8 (Takano et al. 1994; Makishima et al. 2000), NGC 2403 X-3 (Kotoku et al. 2000), and NGC 4449 Source 2 (Miyawaki et al. 2004). Future studies of luminosity-correlated spectral evolution with a larger sample of extragalactic X-ray point sources will elucidate the detailed composition of ULXs.

The authors would like to thank Chris Done for her valuable comments. T. Tanaka is supported by research fellowships of the Japan Society for the Promotion of Science for Young Scientists.

References

- Dickey, J. M., & Lockman, F. J. 1990, ARA&A, 28, 215
 Ebisawa, K., Makino, F., Mitsuda, K., Belloni, T., Cowley, A. P., Schmidtke, P. C., & Treves, A. 1993, ApJ,

- 403, 684
Fabbiano, G. 1989, *ARA&A*, 27, 87
Fabbiano, G., & Trinchieri, G. 1984, *ApJ*, 286, 491
Gierliński, M., & Done, C. 2004, *MNRAS*, 347, 885
Gilfanov, M., Grimm, H. J., & Sunyaev, R. 2004, *Nucl. Phys. B. Proc. Suppl.*, 132, 369
Jansen, F., et al. 2001, *A&A*, 365, L1
Kotoku, J., Mizuno, T., Kubota, A., & Makishima, K. 2000, *PASJ*, 52, 1081
Kubota, A., & Makishima, K. 2004, *ApJ*, 601, 428
Kubota, A., Done, C., & Makishima, K. 2002, *MNRAS*, 337, L11
Kubota, A., Makishima, K., & Ebisawa, K. 2001, *ApJ*, 560, L147
Kubota, A., Tanaka, Y., Makishima, K., Ueda, Y., Dotani, T., Inoue, H., & Yamaoka, K. 1998, *PASJ*, 50, 667
Makishima, K., et al. 2000, *ApJ*, 535, 632
McClintock, J. E., & Remillard, R. A. 2005, in *Compact Stellar X-ray Sources*, ed. Lewin, W. H. G. & van der Klis, M. (Cambridge, UK: Cambridge University Press) in press, astro-ph/0306213
Mitsuda, K., et al. 1984, *PASJ*, 36, 741
Miyawaki, R., Sugiho, M., Kokubun, M., & Makishima, K. 2004, *PASJ*, 56, 591
Mizuno, T., Kubota, A., & Makishima, K. 2001, *ApJ*, 554, 1282
Ogawa, M., 1992, Master Thesis, Rikkyo University
Pietsch W., et al. 2001, *A&A*, 365, L174
Puche, D., & Carignan, C. 1988, *AJ*, 95, 1025
Shakura, N. I., & Sunyaev, R. A. 1973, *A&A*, 24, 337
Shimura, T., & Takahara, F. 1995, *ApJ*, 445, 780
Strickland, D. K., Heckman, T. M., Weaver, K. A., & Dahlem, M. 2000, *AJ*, 120, 2965
Strickland, D. K., Heckman, T. M., Weaver, K. A., Hoopes, C. G., & Dahlem, M. 2002, *ApJ*, 568, 689
Strüder, L., et al. 2001, *A&A*, 365, L18
Sugiho, M. 2003, PhD Thesis, The University of Tokyo
Takano, M., Mitsuda, K., Fukazawa, Y., & Nagase, F. 1994, *ApJ*, 436, L47
Takizawa, M. 1991, Master Thesis, The University of Tokyo
Turner, M. J. L., et al. 2001, *A&A*, 365, L27
Vogler, A., & Pietsch, W. 1999, *A&A*, 342, 101
Weisskopf, M. C., Tananbaum, H. D., Van Speybroeck, L. P., & O'Dell, S. L. 2000, *Proc. SPIE*, 4012, 2
Zycki, P. T., Done, C., & Smith, D. A. 1999, *MNRAS*, 309, 561